Chinese Chemical Letters 31 (2020) 2019–2022

Contents lists available at ScienceDirect

Chinese Chemical Letters

journal homepage: www.elsevier.com/locate/cclet

Communication

Ultrasmall Ru nanoparticles supported on chitin nanofibers for hydrogen production from $NaBH_4$ hydrolysis

Jiapeng Zhang, Fanzhen Lin, Lijing Yang, Zhaoyi He, Xiaoshan Huang, Dingwei Zhang, Hua Dong*

College of Materials and Chemistry & Chemical Engineering, Chengdu University of Technology, Chengdu 610059, China

ARTICLE INFO

Article history:
Received 3 November 2019
Received in revised form 25 November 2019
Accepted 26 November 2019
Available online 27 November 2019

Keywords:
Ru
Chitin
Hydrogen generation
$NaBH_4$
Catalytic hydrolysis

ABSTRACT

In this work, a series of chitin-supported Ru catalysts, composed of ultrasmall Ru nanoparticles supported on the chitin nanofibers, with different Ru content from 0.07 wt% to 0.93 wt%, are fabricated. Results from catalyzed $NaBH_4$ hydrolysis experiments indicate that the catalytic activity of the fabricated chitin-supported Ru catalysts increases gradually with the decreasing of Ru content. The rate of hydrogen generation from $NaBH_4$ hydrolysis catalyzed by the catalyst with 0.07 wt% Ru content is as high as 55.29 L min^{-1} g_{Ru}^{-1} at 30 °C, and this reaction exhibits activation energy of 39.16 kJ/mol. The augment of $NaBH_4$ dosage in the experiments does not weaken the catalytic activity. In addition, the fabricated chitin-supported Ru catalysts show excellent durability in $NaBH_4$ hydrolysis, with only 9.2% activity loss after used for 20 cycles. With excellent catalytic activity and durability, the as-obtained Ru catalysts provide a promising choice for promoting hydrogen production from $NaBH_4$ hydrolysis.

Hydrogen is an environmentally friendly energy source, with a very high energy density and emitting only water after its oxidation [1–3]. In spite of these prominent advantages, the storage and transportation of H_2 is still challenging [2,4]. Therefore, many hydrides which can store hydrogen readily under mild conditions have been developed [5,6]. For example, $NaBH_4$ is a typical safe hydride with reliable stability [7]. It possesses impressive hydrogen storage capacity [8], with the hydrolysis of 1 g $NaBH_4$ producing 0.21 g H_2:

$$NaBH_4 + 2H_2O \xrightarrow{Catalyst} NaBO_2 + 4H_2 \quad (1)$$

Although the amount of H_2 provided by $NaBH_4$ is considerable, it has been well known since its original discovery that the aqueous $NaBH_4$ solution has remarkable stability to hydrolysis [1,9]. Thus, appropriate catalysts with excellent catalytic activity for promoting $NaBH_4$ hydrolysis are highly required.

Herbert C. Brown and Charles A. Brown investigated the catalytic activity of various metal catalysts on the hydrolysis reaction of $NaBH_4$, and found that Ru released H_2 more rapidly than Pt, Pd, Fe, Co, Ni, *etc.* [10]. In the last years, great progress has been made on developing catalysts for $NaBH_4$ hydrolysis [3,11–18]. And many catalysts based on non-noble metals [19–32] or non-metal materials [33,34] with impressive catalytic activity have been reported, while their performance is still below their Ru-based counterparts [35–41]. However, as a noble metal, the scarcity and high cost of Ru are obstacles on the way to industrial applications [3]. It is therefore highly desirable to improve furtherly the catalytic performance of Ru catalysts for $NaBH_4$ hydrolysis. For this reason, Ru catalysts have been widely investigated for decades [3]. Ru nanoparticles, which have high catalytic activity for $NaBH_4$ hydrolysis due to high proportion of surface Ru atoms, have attracted more attention of researchers [42–47]. However, it is well-known that nanoparticles tend to aggregate during catalysis process, resulting in loss of catalytic activity. Therefore, Ru nanoparticles were often deposited on varieties of substrates, such as ZIF-67 nanoparticles [42], graphene [43], Al_2O_3 pellets [44], nickel foam [45], TiO_2 nanoparticles [46] and PEDOT [47], to improve their stability in $NaBH_4$ hydrolysis. These substrates provided promising choices for Ru catalysts, nevertheless, new substrates with special structures, high surface area, and easy fabrication with low cost are still desperately desired.

Chitin is the second most abundant naturally produced biopolymer behind cellulose. It is biodegradable and renewable. Nanofibrous chitin materials could be fabricated through a dissolution-precipitation method with NaOH/urea aqueous solution as solvent [48,49]. This kind of nanofibrous chitin materials has nanoporous structure and high surface area,

* Corresponding author.
E-mail address: donghua@iccas.ac.cn (H. Dong).

https://doi.org/10.1016/j.cclet.2019.11.042
1001-8417/

providing excellent substrates for metal catalysts. In this work, chitin-supported Ru (Ru/chitin) catalysts composed of ultrasmall Ru nanoparticles supported on chitin nanofibrous substrate (Fig. S1 in Supporting information) were fabricated through a cheap and easy method. The structure of the catalysts and their Ru content were investigated with scanning electron microscopy (SEM), transmission electron microscopy (TEM), high-angle annular dark field-scanning transmission electron microscopy (HAADF-STEM), X-ray diffraction (XRD), X-ray photoelectron spectroscopy (XPS), and inductively coupled plasma optical emission spectrometry (ICP-OES). The effects of Ru content of the catalysts, $NaBH_4$ dosage, and reaction temperature on $NaBH_4$ hydrolysis were discussed by measuring H_2 generation rates under different conditions. The experiment results showed that the fabricated catalysts could provide a H_2 generation rate as high as 55.29 L min^{-1} g_{Ru}^{-1} at 30 °C, and showed no significant activity loss after reused for 20 times, indicating excellent catalytic performance.

As shown in Fig. S2 (Supporting information), the chitin substrate used in this work had distinct nanoporous structure. The Brunauer-Emmett-Teller (BET) surface measurement showed that it had a surface area as high as 168 m^2/g, providing huge space for Ru nanoparticles to anchor.

To fabricate the Ru catalysts, Ru^{3+} was firstly adsorbed onto the surface of nanoporous chitin substrate, and then was reduced to Ru nanoparticles. By controlling the amount of Ru^{3+} used during the fabrication process, Ru/chitin catalysts with Ru content of 0.07 wt%, 0.18 wt%, 0.29 wt%, 0.59 wt% and 0.93 wt% were obtained. These catalysts were identified as Ru-0.07, Ru-0.18, Ru-0.29, Ru-0.59, and Ru-0.93 in the following text, respectively.

As shown in Figs. 1a and b, the fabricated Ru/chitin catalysts had distinct nanoporous structure. However, the morphology of the fabricated catalysts was a little different from the raw substrate material (Fig. S2 in Supporting information). It was probably caused by slight aggregation during catalyst fabrication. The backbones of the catalysts had a crosslinked fiber-like structure. The fiber diameter was from tens to hundreds of nanometers, and the size of the nanopores among the fibers was from tens to hundreds of nanometers as well. It was consistent with the adsorption average pore diameter of 66 nm obtained from BET test. This kind of nanoporous fibrous structure had advantages in high surface area and in high porosity. High surface area insured enough space for Ru nanoparticles to anchor, and high porosity guaranteed fast substance exchange between inside and outside of the catalysts. Both the two factors worked together, providing the catalysts with better performance in catalyzing $NaBH_4$ hydrolysis. To confirm the successful anchoring of Ru nanoparticles on the substrate, HAADF-STEM and TEM investigation were carried out and the results were shown in Figs. 1c and d, from which distinct ultrasmall Ru nanoparticles with average diameter as small as 2.4 nm can be clearly observed. The lattice fringes in the inset of Fig. 1d indicated the planes with interplanar spacing of 2.3 Å, corresponding to (100) planes of Ru metal nanoparticles. Furthermore, in XRD pattern of the catalysts (Fig. 2a), the only peaks from 5° to 30° belonged to the chitin substrate [50], while there were no significant reflections associated with metallic Ru species. This could further confirm the small size of Ru nanoparticles. Small nanoparticles could provide more surface atoms, making their catalytic activities improved.

Figs. 2b and c have shown the XPS spectra of the Ru/chitin catalysts. Fig. 2b shows the full survey XPS spectrum of Ru/chitin catalysts with peaks of C, N, O and Ru. The peaks of C, N and O were from nanoporous chitin substrate, whereas the very small peaks of Ru were from Ru nanoparticles. Fig. 2c demonstrates specific 3p peaks of Ru species in the catalysts [51]. Although the intensity was very low, it indeed verified the existence of Ru species in the catalysts.

The rate of H_2 generation from $NaBH_4$ hydrolysis was used to evaluate the catalytic activities of the obtained Ru/chitin catalysts. The experiments were carried out in a home-built set-up (Fig. S3 in Supporting information). The catalysts and $NaBH_4$ solution were mixed in a flask with a final reaction mixture weight of 10 g, and the generated H_2 was collected and measured with a glass burette.

Compared with the reactions uncatalyzed or catalyzed by bare nanoporous chitin, $NaBH_4$ hydrolysis catalyzed by Ru/chitin catalysts had far outstripping H_2 generation rates (Fig. S4 in Supporting information). For different Ru/chitin catalysts, the Ru content of the catalysts had distinct effect on their catalytic activities. Catalyzed $NaBH_4$ hydrolysis experiments were carried

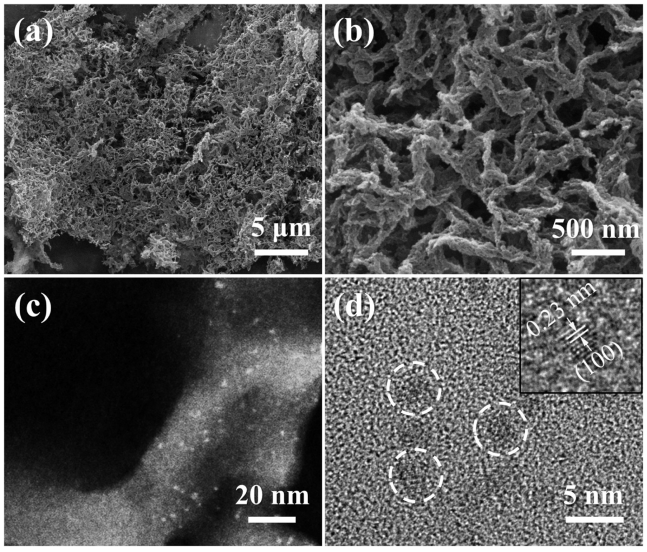

Fig. 1. (a, b) SEM images of Ru-0.07 catalyst. The crosslinked fiber-like backbones of the catalyst provide it with nanoporous structure. (c) HAADF-STEM image and (d) high resolution TEM images of Ru-0.07 catalyst. Well-distributed ultrasmall Ru nanoparticles can be clearly observed. Several nanoparticles are circled for conspicuousness in (d). The lattice fringes in the inset of (d) show interplanar spacing of 2.3 Å, corresponding to (100) planes of Ru metal nanoparticles.

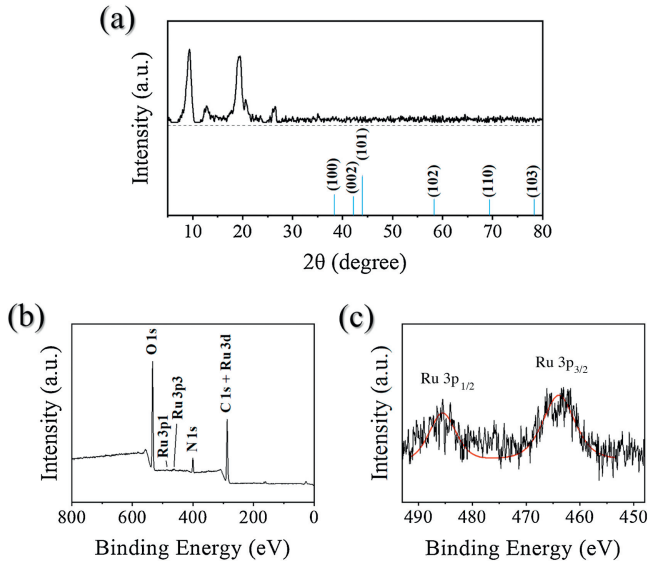

Fig. 2. (a) XRD pattern of Ru/chitin catalysts (top) and standard XRD pattern of metallic Ru (bottom). The chitin peaks from 5° to 30° are distinct, while no reflections associated with metallic Ru species can be observed. (b, c) XPS analysis of Ru/chitin catalysts: (b) Full survey XPS spectrum shows very small peaks of Ru and distinct peaks of C, N and O; (c) Partial scan shows specific peaks of Ru 3p.

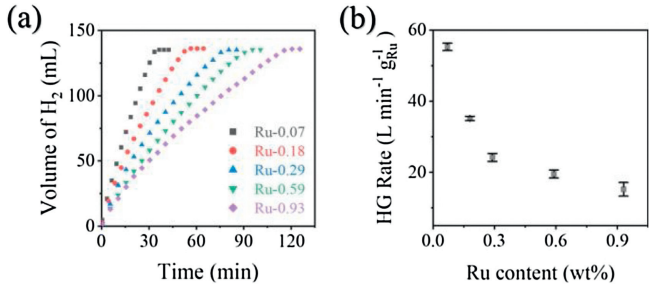

Fig. 3. H_2 generation from $NaBH_4$ hydrolysis catalyzed by Ru/chitin catalysts with different Ru content. (a) Plots of H_2 volume *versus* time for reactions catalyzed by different catalysts. (b) H_2 generation (HG) rate per gram Ru decreases dramatically with the increase of Ru content in the catalysts. Experiment conditions: 10 g reaction mixture, 50 mg $NaBH_4$, 30 °C.

out to disclose the difference among the catalytic activities. For the experiments of Ru-0.07 catalyst, 100 mg catalyst was used for each experiment, while for the other catalysts, the amount of Ru species was controlled the same as in the experiments of Ru-0.07. As shown in Fig. 3, although the amount of Ru was the same for each catalyst, their catalytic activities were distinctly different. The catalytic activity increased dramatically with the decreasing of Ru content in the catalysts. Ru-0.07 catalyst, with Ru content of 0.07 wt%, had the best catalytic activity, giving a H_2 generation rate of 55.29 L min^{-1} g_{Ru}^{-1}. This value is comparable with the best results reported recently (Table S1 in Supporting information) [38–44]. With the increasing of Ru content, however, the catalytic activity gradually decreased. For Ru-0.93 with Ru content of 0.93 wt%, the H_2 generation rate decreased to 15.21 L min^{-1} g_{Ru}^{-1}, with 72.5% decrease compared with Ru-0.07. This was probably caused by the different distribution of Ru nanoparticles. Compared with the nanoparticles in the catalysts with higher Ru content (Fig. S5a in Supporting information), Ru nanoparticles were smaller and distributed better in the catalysts with lower Ru content (Fig. S5b in Supporting information), with more surface Ru atoms capable of catalyzing $NaBH_4$ hydrolysis, resulting in better catalytic activity [36,42].

The effect of $NaBH_4$ concentration on the H_2 generation rate was shown in Fig. S6 (Supporting information). From the slopes of the lines, it can be clearly seen that the catalytic activity of Ru-0.07 was not decreased when amount of $NaBH_4$ used increased from 25 mg to 500 mg. The H_2 generation rate actually increased slightly with the increasing of $NaBH_4$ amount, especially from 125 mg to 500 mg. When $NaBH_4$ amount reached 1 g (10 wt% concentration), the initial H_2 generation rate was high too; however, it dropped down in a short time after the reaction started (brown stars in Fig. S6). When the $NaBH_4$ concentration was too high, the solution became too viscous. The byproduct of hydrolysis, $NaBO_2$, could not diffuse quickly, so it deposited on the catalysts, blocking the way for reactants to reach the catalysts [38,42]. As a result, the H_2 generation rate decreased dramatically. Additionally, when the amount of $NaBH_4$ used was from 25 mg to 500 mg, the final volume of H_2 generated was proportional to the amount of $NaBH_4$ used. It suggests that the change of $NaBH_4$ amount in this range did not have significant negative effect on the catalytic activity of the catalysts for $NaBH_4$ hydrolysis.

Another important factor which drastically influenced H_2 generation rate was temperature. The H_2 generation tests catalyzed by Ru-0.07 were carried out at different temperature from 30 °C to 70 °C. It can be clearly observed from Fig. 4a that H_2 generation was accelerated sharply with temperature increasing. Compared with the H_2 generation rate of 55.29 L min^{-1} g_{Ru}^{-1} at 30 °C, it increased by 5.66 times to 313.10 L min^{-1} g_{Ru}^{-1} at 70 °C (Fig. S7 in Supporting information). The activation energy (E_a) of H_2

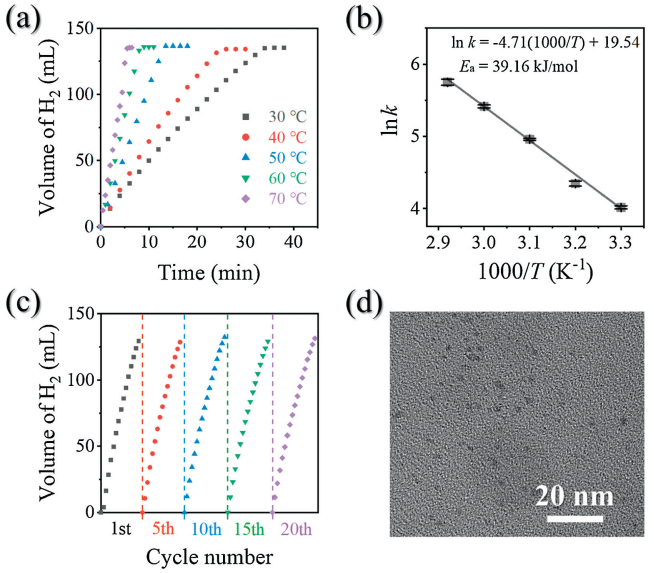

Fig. 4. (a, b) H_2 generation from $NaBH_4$ hydrolysis catalyzed by Ru-0.07 at different reaction temperature: (a) Plots of H_2 volume *versus* time for reactions catalyzed by Ru-0.07 catalyst at different reaction temperature; (b) Arrhenius plot for Ru-0.07 catalyzed $NaBH_4$ hydrolysis. Experiment conditions: 10 g reaction mixture, 50 mg $NaBH_4$, 100 mg Ru-0.07. (c, d) The durability of Ru-0.07 in cycle use: (c) Ru-0.07 catalyst shows very little activity loss after used for 20 cycles; (d) TEM image of Ru-0.07 catalyst after used for 20 cycles. Experiment conditions: 10 g reaction mixture, 50 mg $NaBH_4$, 100 mg Ru-0.07, 30 °C.

generation reaction is an important reference to evaluate catalyst performance. Therefore, the E_a of Ru-0.07 catalyzed H_2 generation reaction was calculated according to Arrhenius equation:

$$\ln k = \ln A - E_a/RT \quad (2)$$

where T is H_2 generation reaction temperature in Kelvin (K), k is the corresponding rate constant of reactions, R is the gas constant, and A is pre-exponential factor. Based on the results of H_2 generation reactions catalyzed by Ru-0.07 at different temperature, the E_a was calculated at about 39.16 kJ/mol (Fig. 4b), which is comparable with the activation energy of many $NaBH_4$ hydrolysis reactions catalyzed by other Ru catalysts (Table S1) [38–43]. It indicates that Ru-0.07 had remarkable catalytic activity for H_2 generation from $NaBH_4$ hydrolysis.

If a catalyst is going to be used in practical application, the reusability must be satisfying. In the present study, the reusability of Ru-0.07 was evaluated by measuring its activity in cycle use. After each $NaBH_4$ hydrolysis reaction, the catalyst was collected by centrifugation, washed thoroughly with water, and dispersed in water again for next use. As shown in Fig. 4c, Ru-0.07 catalyst did not show significant activity loss after 20 cycles of experiments. The calculated H_2 generation rate at 20th cycle was 90.8% of that at the 1st cycle. The TEM image (Fig. 4d) has shown that there were still distinct ultrasmall nanoparticles well-distributed on the chitin substrate in the Ru-0.07 catalyst which had been used for 20 times. The good reusability can be partially ascribed to the stability of the catalyst itself, while the thorough wash of the catalyst can be another reason. As mentioned above, the byproduct of $NaBH_4$ hydrolysis, $NaBO_2$, which remains on the surface of catalysts, can block the way for reactants to reach the catalysts, resulting in decreasing of catalytic activity. Indeed, in our experiments, if the catalysts were not washed, the H_2 generation rate could decrease distinctly. Fortunately, the chitin substrate had a surface very hydrophilic. During washing with water, mass exchange on the catalyst surface was easy and smooth. Therefore, the catalyst could be washed thoroughly after each use, bringing back the original catalytic activity successfully.

Through a cheap and easy method, chitin-supported Ru catalysts, composed of ultrasmall Ru nanoparticles supported on nanoporous chitin substrate, with Ru content from 0.07 wt% to 0.93 wt% were successfully fabricated. SEM investigation showed that the catalysts had nanoporous structure and crosslinked fiber-like backbones. TEM investigation showed that Ru nanoparticles were ultrasmall and well distributed on chitin substrate. By comparing the catalysts with different Ru content, it was found that the catalytic activity for $NaBH_4$ hydrolysis gradually increased with the decreasing of Ru content. Ru-0.07 catalyst (0.07 wt% Ru content) showed a H_2 generation rate of 55.29 L min^{-1} g_{Ru}^{-1} at 30 °C, nearly 4 times as high as that of Ru-0.93 (0.93 wt% Ru content). The E_a of $NaBH_4$ hydrolysis catalyzed by Ru-0.07 was calculated as 39.16 kJ/mol. Moreover, the fabricated catalysts showed excellent reusability, with only 9.2% activity loss after used for 20 times. The results indicate that the developed catalysts have excellent catalytic performance for catalyzing $NaBH_4$ hydrolysis, providing a promising choice for promoting H_2 production.

Declaration of competing interest

The authors declare that they have no known competing financial interests or personal relationships that could have appeared to influence the work reported in this paper.

Acknowledgment

This work was supported by Chengdu University of Technology (No. 10912-2019KYQD07208).

Appendix A. Supplementary data

Supplementary material related to this article can be found, in the online version, at doi:https://doi.org/10.1016/j.cclet.2019.11.042.

References

[1] S.S. Muir, X.D. Yao, Int. J. Hydrogen Energy 36 (2011) 5983–5997.
[2] A.M. Abdalla, S. Hossain, O.B. Nisfindy, et al., Energy Convers. Manage. 165 (2018) 602–627.
[3] P. Brack, S.E. Dann, K.G.U. Wijayantha, Energy Sci. Eng. 3 (2015) 174–188.
[4] A. Schneemann, J.L. White, S. Kang, et al., Chem. Rev. 118 (2018) 10775–10839.
[5] T.P. Huang, J.X. Zou, N. Zhao, X.Q. Zeng, W.J. Ding, J. Alloys Compd. 791 (2019) 1270–1276.
[6] Y.N. Men, J. Su, X.L. Wang, et al., Chin. Chem. Lett. 30 (2019) 634–637.
[7] L.Z. Ouyang, W. Chen, J.W. Liu, et al., Adv. Energy Mater. 7 (2017) 1700299.
[8] D.M.F. Santos, C.A.C. Sequeira, Renew. Sust. Energy Rev. 15 (2011) 3980–4001.
[9] H.I. Schlesinger, H.C. Brown, A.E. Finholt, et al., J. Am. Chem. Soc. 75 (1953) 215–219.
[10] H.C. Brown, C.A. Brown, J. Am. Chem. Soc. 84 (1962) 1493–1494.
[11] S.H. Wang, Y.A. Fan, M.Q. Chen, et al., J. Mater. Chem. A 3 (2015) 8250–8255.
[12] X.C. Shen, Q. Wang, Q.Q. Wu, et al., Energy 90 (2015) 464–474.
[13] A. Zabielaite, A. Balciunaite, I. Stalnioniene, et al., Int. J. Hydrogen Energy 43 (2018) 23310–23318.
[14] J. Guo, Y.J. Hou, B. Li, Y.L. Liu, Int. J. Hydrogen Energy 43 (2018) 15245–15254.
[15] H.K. Cai, L.P. Liu, Q. Chen, P. Lu, J. Dong, Energy 99 (2016) 129–135.
[16] H. Jia, X.J. Liu, X. Chen, et al., Int. J. Hydrogen Energy 42 (2017) 28425–28433.
[17] H.M. Sun, J. Meng, L.F. Jiao, F.Y. Cheng, J. Chen, Inorg. Chem. Front. 5 (2018) 760–772.
[18] N. Patel, A. Miotello, Int. J. Hydrogen Energy 40 (2015) 1429–1464.
[19] X.Y. Zhang, X.W. Sun, D.Y. Xu, et al., Appl. Surf. Sci. 469 (2019) 764–769.
[20] M. Bekirogullari, M. Kaya, C. Saka, Int. J. Hydrogen Energy 44 (2019) 7262–7275.
[21] J.Z. Ding, Q. Li, Y. Su, et al., Int. J. Hydrogen Energy 43 (2018) 9978–9987.
[22] Z.T. Gao, C.M. Ding, J.W. Wang, et al., Int. J. Hydrogen Energy 44 (2019) 8365–8375.
[23] L. Hostert, E.G.C. Neiva, A.J.G. Zarbin, E.S. Orth, J. Mater. Chem. A 6 (2018) 22226–22233.
[24] T.T. Liu, K.Y. Wang, G. Du, A.M. Asiri, X.P. Sun, J. Mater. Chem. A 4 (2016) 13053–13057.
[25] C. Luo, F.Y. Fu, X.J. Yang, et al., ChemCatChem 11 (2019) 1643–1649.
[26] M.X. Ma, L. Wei, F. Jin, Funct. Mater. Lett. 12 (2019) 1850109.
[27] A.M. Pornea, M.W. Abebe, H. Kim, Chem. Phys. 516 (2019) 152–159.
[28] G.R.M. Tomboc, A.H. Tamboli, H. Kim, Energy 121 (2017) 238–245.
[29] F.H. Wang, Y.J. Zhang, Y.A. Wang, et al., Int. J. Hydrogen Energy 43 (2018) 8805–8814.
[30] Y. Wang, W. Meng, D. Wang, et al., Int. J. Hydrogen Energy 42 (2017) 30718–30726.
[31] H.M. Zhang, X.L. Feng, L.N. Cheng, et al., Colloid Surf. A 563 (2019) 112–119.
[32] Y.N. Men, J. Su, C.Z. Huang, et al., Chin. Chem. Lett. 29 (2018) 1671–1674.
[33] L.L. Lu, H.J. Zhang, S.W. Zhang, F.L. Li, Angew. Chem. Int. Ed. 54 (2015) 9328–9332.
[34] N. Sahiner, Int. J. Hydrogen Energy 43 (2018) 9687–9695.
[35] N. Cao, W. Luo, G.Z. Cheng, Int. J. Hydrogen Energy 38 (2013) 11964–11972.
[36] J.Y. Guo, C.B. Wu, J.F. Zhang, et al., J. Mater. Chem. A 7 (2019) 8865–8872.
[37] L. Wen, Z. Zheng, W. Luo, P. Cai, G.Z. Cheng, Chin. Chem. Lett. 26 (2015) 1345–1350.
[38] Y.S. Wei, Y. Wang, L. Wei, et al., Int. J. Hydrogen Energy 43 (2018) 592–600.
[39] M. Wen, Y.Z. Sun, X.M. Li, et al., J. Power Sources 243 (2013) 299–305.
[40] G. Bozkurt, A. Ozer, A.B. Yurtcan, Energy 180 (2019) 702–713.
[41] Y. Liang, H.B. Dai, L.P. Ma, P. Wang, H.M. Cheng, Int. J. Hydrogen Energy 35 (2010) 3023–3028.
[42] D.D. Tuan, K.Y.A. Lin, Chem. Eng. J. 351 (2018) 48–55.
[43] M.H. Tan, Y. Wang, A. Taguchi, et al., Int. J. Hydrogen Energy 44 (2019) 7320–7325.
[44] Y.H. Huang, C.C. Su, S.L. Wang, M.C. Lu, Energy 46 (2012) 242–247.
[45] Z.M. Huang, A. Su, Y.C. Liu, Energy 51 (2013) 230–236.
[46] K. Mori, K. Miyawaki, H. Yamashita, ACS Catal. 6 (2016) 3128–3135.
[47] A.D. Chowdhury, N. Agnihotri, A. De, Chem. Eng. J. 264 (2015) 531–537.
[48] B. Duan, X. Zheng, Z.X. Xia, et al., Angew. Chem. Int. Ed. 54 (2015) 5152–5156.
[49] B. Duan, Y. Huang, A. Lu, L.N. Zhang, Prog. Polym. Sci. 82 (2018) 1–33.
[50] G. Cardenas, G. Cabrera, E. Taboada, S.P. Miranda, J. Appl. Polym. Sci. 93 (2004) 1876–1885.
[51] D.J. Morgan, Surf. Interface Anal. 47 (2015) 1072–1079.